Journal of Solid Mechanics Vol. 3, No. 2 (2011) pp. 183-197

A Power Series Solution for Free Vibration of Variable Thickness Mindlin Circular Plates with Two-Directional Material Heterogeneity and Elastic Foundations

M.M. Alipour, M. Shariyat*

Faculty of Mechanical Engineering, K.N. Toosi University of Technology, Tehran 19991-43344, Iran

Received 31 May 2011; accepted 15 July 2011

ABSTRACT

In the present paper, a semi-analytical solution is presented for free vibration analysis of circular plates with complex combinations of the geometric parameters, edge-conditions, material heterogeneity, and elastic foundation coefficients. The presented solution covers many engineering applications. The plate is assumed to have a variable thickness and made of a heterogeneous material whose properties vary in both radial and transverse directions. While the edge is simply-supported, clamped, or free; the bottom surface of the plate is resting on a two-parameter (*Winkler-Pasternak*) elastic foundation. A comprehensive sensitivity analysis including evaluating effects of various parameters is carries out. *Mindlin* theory is employed for derivation of the governing equations whereas the differential transform method is used to solve the resulted equations. In this regard, both the in-plane and rotary inertia are considered. Results show that degradations caused by a group of the factors (e.g., the geometric parameters) in the global behavior of the structure may be compensated by another group of factors of different nature (e.g, the material heterogeneity parameters). Moreover, employing the elastic foundation leads to higher natural frequencies and postponing the resonances.

Keywords: Free vibration; Circular plate; Elastic foundation; Two-directional functionally graded material; Variable thickness; Differential transform.

1 INTRODUCTION

MANY engineering components may be modeled as circular plates with uniform or variable thickness. Some of the circular components may be supported by spring elements, elastic foundations or shearing pads (e.g., the driven plate of a friction). There are some research works on free vibration of isotropic circular and annular plates resting on elastic foundations [1, 2]. Some researchers such as Ramaiah and Vijayakumar [3], Narita [4], and Lin and Tseng [5] studied the annular orthotropic plates.

Due to the abrupt changes in the material properties of the composite materials and subsequently, possibility of local failure occurrence, functionally graded materials have been used as alternative materials in some applications. Functionally graded materials provide the capability to accurately monitor local variations of the material properties to meet the strength or other design criteria at the continuum scale, especially when multidirectional functionally graded materials are employed. Using the first-order shear-deformation theory (FSDT), Prakash and Ganapathi [6] investigated asymmetric free vibration characteristics of the functionally graded circular plates. Efraim and

* Corresponding author. Tel.: +98 912 272 7199; Fax: +98 21 8867 4748.
E-mail address: m_shariyat@yahoo.com and *shariyat@kntu.ac.ir* (M. Shriyat).

Eisenberger [7] presented vibration analysis of the variable thickness thick annular isotropic and functionally graded plates using the FSDT. Nie and Zhong [8] proposed a semi-analytical method for free and forced vibration analyses of functionally graded circular plates with various boundary conditions. Dong [9] investigated the three-dimensional free vibration of the functionally graded annular plates. A free vibration analysis of thick functionally graded plates supported by elastic foundations was presented by Malekzadeh [10], using the differential quadrature method and a series solution. Wang et al. [11] investigated the free axisymmetric vibration of functionally graded plates whose material properties obey an exponential law along the thickness direction, based on the three-dimensional theory. Nie and Zhong [12] presented dynamic analysis of the multi-directional functionally graded annular plates using a state space-based differential quadrature method based on the three-dimensional elastic theory and assuming the material properties to vary according to an exponent law along the thickness and radial directions.

The differential transform method (DTM) is a semi-analytical technique that has been proposed based on Taylor's series. Employing DTM, it is possible to obtain highly convergent and accurate solutions for the differential or integro-differential equations [13]. By using this method, the governing differential equations can be reduced to recurrence relations and the boundary conditions may be transformed into a set of algebraic equations. Some researchers have successfully used the DTM in solving the eigenvalue problems [14, 15]. Yeh et al. [16] analyzed free vibration of the rectangular thin plates, using a hybrid method which combines the finite difference and the differential transformation methods. Yeh et al. [17] studied large deflections of an orthotropic rectangular thin plate employing a similar hybrid method. Yalcin [18] analyzed free vibration of thin circular plates with various boundary conditions, using the differential transform method. Shariyat and Alipour [19] and Alipour et al. [20] investigated free vibration of the two-directional functionally graded circular plates based on the differential transformation method and the classical plate theory.

The above review reveals that vibration analysis of circular plates with two-directionally graded materials almost has not been performed by other researchers. In the present paper, employing *Mindlin*'s first-order shear-deformation plate theory, the differential transformation method is employed to develop a series solution for free vibration of two-directional functionally graded circular plates with variable thickness on elastic two-parameter (*Winkler-Pasternak*) foundations. Both in-plane and rotary moments of inertia are taken into account. Various edge conditions are considered in the present analysis and some practical conclusions are inferred.

2 MATHEMATICAL FORMULATIONS

2.1 The governing equations of motion

Based on *Mindlin*'s plate theory, displacement field of the plate may be described as follows [21]:

$$u = u_0 + z\psi_r, \qquad v = v_0 + z\psi_\theta, \qquad w = w_0 \tag{1}$$

where the symbol "," stands for the partial derivative and u_0, v_0, and w_0 are the radial, circumferential, and transverse displacement components of the reference layer (e.g. the mid-surface) of the circular plate, respectively and the coordinate z is measured from the reference layer and is positive upward. ψ_r is rotation of the normal to the middle surface in the radial plane. For small deflections, the strain-displacement relations may be written as [21]:

$$\varepsilon_r = u_{,r}, \qquad \varepsilon_\theta = \frac{u}{r} + \frac{v_{,\theta}}{r}, \qquad \varepsilon_{r\theta} = v_{,r} + \frac{u_{,\theta}}{r} - \frac{v}{r}, \qquad \varepsilon_{rz} = u_{,z} + w_{,r}, \qquad \varepsilon_{\theta z} = v_{,z} + \frac{w_{,\theta}}{r} \tag{2}$$

On the other hand, as a consequence of the assumptions of *Mindlin*'s plate theory, Hooke's generalized stress-strain law may be expressed as [22]:

$$\begin{aligned} &\sigma_r = \frac{E}{1-\nu^2}(\varepsilon_r + \nu\varepsilon_\theta), \qquad \sigma_\theta = \frac{E}{1-\nu^2}(\varepsilon_\theta + \nu\varepsilon_r), \qquad \sigma_{r\theta} = \frac{E}{2(1+\nu)}\varepsilon_{r\theta} \\ &\sigma_{rz} = \kappa^2 \frac{E}{2(1+\nu)}\varepsilon_{rz}, \qquad \sigma_{\theta z} = \kappa^2 \frac{E}{2(1+\nu)}\varepsilon_{\theta z} \end{aligned} \tag{3}$$

where k^2 denotes the transverse shear correction factor which is usually introduced in the first-order shear-deformation plate/shell theories in order to improve the transverse shear rigidity of the plate. In the present analysis, this coefficient is adopted as $\kappa^2 = \pi^2/12$ [21].

The governing equations of motion may be derived by using *Hamilton's principle*. Employing this principle leads to the following three equations of motion for the plate under consideration in the cylindrical coordinate system (r, θ, z) [22]:

$$N_{r,r} + \frac{N_r - N_\theta}{r} = I_0\ddot{u}_0 + I_1\ddot{\psi}_r \tag{4a}$$

$$M_{r,r} + \frac{1}{r}(M_r - M_\theta) - Q_r = I_1\ddot{u}_0 + I_2\ddot{\psi}_r \tag{4b}$$

$$Q_{r,r} + \frac{1}{r}Q_r = I_0\ddot{w} + k_w w - k_s\left(w,_{rr} + \frac{1}{r}w,_r\right) \tag{4c}$$

The stress resultants M_i, N_i, Q_i (i=r, θ) and the moments of inertia I_i (i=0, 1, 2) are defined as [21]:

$$\begin{Bmatrix} M_r \\ M_\theta \end{Bmatrix} = \int_{-h/2}^{h/2} \begin{Bmatrix} \sigma_r \\ \sigma_\theta \end{Bmatrix} z\mathrm{d}z, \qquad \begin{Bmatrix} N_r \\ N_\theta \end{Bmatrix} = \int_{-h/2}^{h/2} \begin{Bmatrix} \sigma_r \\ \sigma_\theta \end{Bmatrix} \mathrm{d}z, \qquad Q_r = \int_{-h/2}^{h/2} \sigma_{rz}\mathrm{d}z \tag{5a}$$

$$\begin{Bmatrix} I_0 \\ I_1 \\ I_2 \end{Bmatrix} = \int_{-h/2}^{h/2} \rho \begin{Bmatrix} 1 \\ z \\ z^2 \end{Bmatrix} \mathrm{d}z \tag{5b}$$

Now consider a circular plate with a two-directional heterogeneity, outer radius b, and a variable thickness h, resting on a two parameter (*Winkler-Pasternak*) elastic foundation. Young's modulus E and the density ρ of the materials are considered to vary in both radial and transverse directions. The geometric as well as the foundation parameters of the circular plate are shown in Fig.1 Variations of Young's modulus, material density ρ, and thickness of the plate are adopted as follows:

$$\begin{aligned} E(r,z) &= [(E_m - E_c)V_f(z) + E_c]e^{\mu\frac{r}{b}}, \\ \rho(r,z) &= [(\rho_m - \rho_c)V_f(z) + \rho_c]e^{\eta\frac{r}{b}}, \\ h &= h_0 e^{\beta\frac{r}{b}} \end{aligned} \tag{6}$$

where the subscripts m and c represent the metallic and ceramic constituents, respectively, and the volume fraction V_f may be given as [20]:

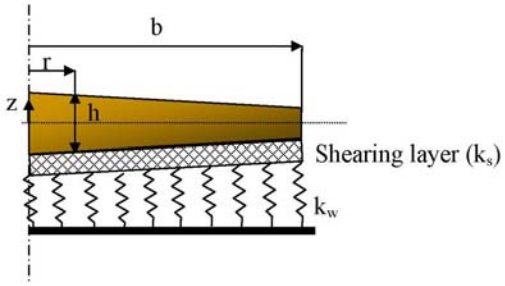

Fig. 1
Geometry and foundation parameters of the two-directional functionally graded variable thickness circular plate.

$$V_f = \left(\frac{z}{h}+\frac{1}{2}\right)^g \tag{7}$$

where g is a positive definite exponent called the power-law index. Greater g values imply that volume fraction of the ceramic constituent material is greater in the FGM mixture. Therefore, based on Eqs. (1)-(6), one may write:

$$\begin{aligned}
M_r &= \left(u_{0,r}+\nu\frac{u_0}{r}\right)B+\left(\psi_r{}_{,r}+\nu\frac{\psi_r}{r}\right)D\\
M_\theta &= B(r)\left(\frac{u_0}{r}+\nu u_{0,r}\right)+D(r)\left(\frac{\psi_r}{r}+\nu\psi_r{}_{,r}\right)\\
N_r &= A(r)\left(u_{0,r}+\nu\frac{u_0}{r}\right)+B(r)\left(\psi_r{}_{,r}+\nu\frac{\psi_r}{r}\right)\\
N_\theta &= A(r)\left(\frac{u_0}{r}+\nu u_{0,r}\right)+B(r)\left(\frac{\psi_r}{r}+\nu\psi_r{}_{,r}\right)\\
Q_r &= \frac{\kappa^2(1-\nu)}{2}A(r)(\psi_r+w_{,r})\\
I_0 &= \overline{I}_0(g)\rho_c h_0 e^{r(\eta+\beta)}\\
I_1 &= \overline{I}_1(g)\rho_c h_0^2 e^{r(\eta+2\beta)}\\
I_2 &= \overline{I}_2(g)\rho_c h_0^3 e^{r(\eta+3\beta)}
\end{aligned} \tag{8}$$

where

$$\begin{aligned}
A(r) &= \int_{-h/2}^{h/2}\frac{E}{1-\nu^2}dz = \frac{E_c}{1-\nu^2}\overline{A}(g)h_0 e^{r(\mu+\beta)}\\
B(r) &= \int_{-h/2}^{h/2}\frac{E}{1-\nu^2}zdz = \frac{E_c}{1-\nu^2}\overline{B}(g)h_0^2 e^{r(\mu+2\beta)}\\
D(r) &= \int_{-h/2}^{h/2}\frac{E}{1-\nu^2}z^2dz = \frac{E_c}{1-\nu^2}\overline{D}(g)h_0^3 e^{r(\mu+3\beta)}
\end{aligned} \tag{9}$$

when the circular plate vibrats with a natural frequency ω, it is possible to separate the time dependence, based on a *Kantorovich-type* approximation [19]:

$$\begin{aligned}
u_0 &= u_0(r)e^{\mathrm{i}\omega t}\\
w &= w(r)\,e^{\mathrm{i}\omega t}\\
\psi_r &= \psi_r(r)e^{\mathrm{i}\omega t}
\end{aligned} \tag{10}$$

$\mathrm{i}=(\sqrt{-1})$ is the imaginary number. To present a more general solution, the following non-dimensional parameters are introduced:

$$\chi=\frac{r}{b},\quad \overline{w}=\frac{w}{b},\quad \tau=\frac{h_0}{b},\quad D^*=\frac{E_c{h_0}^3}{12(1-\nu^2)},\quad K_s=\frac{k_s b^2}{D^*},\quad K_w=\frac{k_w b^4}{D^*},\quad \Omega=\sqrt{\frac{\rho_c h_0}{D^*}}b^2\omega \tag{11}$$

where Ω is the non-dimensional natural frequency. K_w and K_s are the non-dimensional *Winkler* and *Pasternak* coefficients of the elastic foundation, respectively. In the remaining of the paper, the bar ($-$) symbol will not be

shown for the sake of simplicity. The governing Eqs. (4a- 4c) may be simplified and rewritten based on Eqs. (8) and (9) as:

$$\left(u_{0,\chi}+\nu\frac{u_0}{\chi}\right)(\mu+\beta)\overline{A}(g)e^{\chi(\mu+\beta)}+\left(\psi_\chi{}_{,\chi}+\nu\frac{\psi_r}{\chi}\right)(\mu+2\beta)\overline{B}(g)\tau e^{\chi(\mu+2\beta)}$$
$$+\left(u_{0,\chi\chi}+\nu\frac{u_{0,\chi}}{\chi}-\nu\frac{u_0}{\chi^2}\right)\overline{A}(g)e^{\chi(\mu+\beta)}+\left(\psi_r{}_{,\chi\chi}+\nu\frac{\psi_{r,\chi}}{\chi}-\nu\frac{\psi_r}{\chi^2}\right)\overline{B}(g)\tau e^{\chi(\mu+2\beta)}$$
$$+\frac{(1-\nu)}{\chi}\left[\left(u_{0,\chi}-\frac{u_0}{\chi}\right)\overline{A}(g)e^{\chi(\mu+\beta)}+\left(\psi_r{}_{,\chi}-\frac{\psi_r}{\chi}\right)\overline{B}(g)\tau e^{\chi(\mu+2\beta)}\right]$$
$$=-\Omega^2\overline{I}_0(g)e^{\chi(\eta+\beta)}\frac{\tau}{12}u_0-\Omega^2\overline{I}_1(g)\frac{\tau^3}{12}e^{\chi(\eta+2\beta)}\psi_r \tag{12a}$$

$$\left(u_{0,\chi}+\nu\frac{u_0}{\chi}\right)(\mu+2\beta)\overline{B}(g)e^{\chi(\mu+2\beta)}+\left(\psi_r{}_{,\chi}+\nu\frac{\psi_r}{\chi}\right)(\mu+3\beta)\overline{D}(g)\tau e^{\chi(\mu+3\beta)}$$
$$+\left(u_{0,\chi\chi}+\nu\frac{u_{0,\chi}}{\chi}-\nu\frac{u_0}{\chi^2}\right)\overline{B}(g)e^{\chi(\mu+2\beta)}+\left(\psi_r{}_{,\chi\chi}+\nu\frac{\psi_{r,\chi}}{\chi}-\nu\frac{\psi_r}{\chi^2}\right)\overline{D}(g)\tau e^{\chi(\mu+3\beta)}$$
$$+\frac{(1-\nu)}{\chi}\left[\left(u_{0,\chi}-\frac{u_0}{\chi}\right)\overline{B}(g)e^{\chi(\mu+2\beta)}+\left(\psi_r{}_{,\chi}-\frac{\psi_r}{\chi}\right)\overline{D}(g)\tau e^{\chi(\mu+3\beta)}\right]$$
$$-\frac{\kappa^2(1-\nu)}{2}(\psi_r+w_{,\chi})\frac{1}{\tau}\overline{A}(g)e^{\chi(\mu+\beta)}=-\Omega^2\frac{\tau^2}{12}\overline{I}_1(g)e^{\chi(\eta+2\beta)}u_0-\Omega^2\overline{I}_2(g)\frac{\tau^3}{12}e^{\chi(\eta+3\beta)}\psi_r \tag{12b}$$

$$(\psi_{r,\chi}+w_{,\chi\chi})\overline{A}(g)e^{\chi(\mu+\beta)}+(\psi_r+w_{,\chi})(\mu+\beta)\overline{A}(g)e^{\chi(\mu+\beta)}+\frac{\overline{A}(g)e^{\chi(\mu+\beta)}}{\chi}(\psi_r+w_{,\chi})$$
$$=-\frac{1}{6\kappa^2(1-\nu)}\Omega^2\overline{I}_0(g)e^{\chi(\eta+\beta)}\tau^2w+\frac{K_w\tau^2}{6\kappa^2(1-\nu)}w-\frac{K_s\tau^2}{6\kappa^2(1-\nu)}\left(w_{,\chi\chi}+\frac{1}{\chi}w_{,\chi}\right) \tag{12c}$$

2.2 Boundary conditions

The most common edge conditions of the solid circular plates may be expressed as follows:

Free edge: $M_r=0,\quad N_r=0,\quad Q_r=0$ (13a)

Simply-supported edge: $u=0,\quad M_r=0,\quad w=0$ (13b)

Clamped edge: $u=0,\quad w=0,\quad \psi_r=0$ (13c)

3 THE SOLUTION PROCEDURE

3.1 Transformation of the governing equations

By using Taylor's series expansion, the governing differential equations and the relevant boundary conditions of the system are transformed into a set of algebraic equations in terms of the differential transforms of the original functions. Solution of these algebraic equations gives the desired solution of the problem. The basic definitions and the procedure of employing the method are introduced in the present section. Consider functions

$u_0(\chi),\ w(\chi),\ \psi(\chi)$ which are continuous and analytic in a domain R and let $\chi = \chi_0$ represent any point in R. The functions $u_0(\chi),\ w(\chi),\ \psi(\chi)$ may be expressed by a power series whose centers are located at $\chi = \chi_0$.

$$u_0(\chi) = \sum_{k=0}^{\infty} (\chi - \chi_0)^k U_k, \qquad w(r) = \sum_{k=0}^{\infty} (\chi - \chi_0)^k W_k, \qquad \psi_r(\chi) = \sum_{k=0}^{\infty} (\chi - r_0)^k F_k \tag{14}$$

In practical applications, a function may be usually expressed by a finite series. Therefore, Eq. (14) may be rewritten as

$$u_0(r) = \sum_{k=0}^{N} (r - r_0)^k U_k, \qquad w(r) = \sum_{k=0}^{N} (r - r_0)^k W_k, \qquad \psi(r) = \sum_{k=0}^{N} (r - r_0)^k F_k \tag{15}$$

which implies that $u_0(\chi) = \sum_{k=N+1}^{\infty} (\chi - \chi_0)^k U_k$, $w(\chi) = \sum_{k=N+1}^{\infty} (\chi - \chi_0)^k W_k$, and $\psi_r(\chi) = \sum_{k=N+1}^{\infty} (\chi - \chi_0)^k F_k$ are negligibly small. In the present research, value of N is so chosen that the calculated natural frequencies converge.

By substituting Eq. (15) into the governing Eq. (12), the transformed form of this equation around $\chi_0 = 0$, using Taylor's expansion of the exponential functions, may be obtained as:

$$\begin{aligned}
&\sum_{k=0}^{\infty} \Big\{ \overline{A}(g) \sum_{j=0}^{\infty} \frac{(\mu+\beta)^{j+1}}{j!} (k+\nu) U_k \chi^{k+j-1} + \overline{B}(g)\tau \sum_{j=0}^{\infty} \frac{(\mu+2\beta)^{j+1}}{j!} (k+\nu) F_k \chi^{k+j-1} \\
&+ \overline{A}(g) \sum_{j=0}^{\infty} \frac{(\mu+\beta)^{j}}{j!} (k-1)(k+\nu) U_k \chi^{k+j-2} + \overline{B}(g)\tau \sum_{j=0}^{\infty} \frac{(\mu+2\beta)^{j}}{j!} (k-1)(k+\nu) F_k \chi^{k+j-2} \\
&+ (1-\nu)\overline{A}(g) \sum_{j=0}^{\infty} \frac{(\mu+\beta)^{j}}{j!} (k-1) U_k \chi^{k+j-2} + (1-\nu)\overline{B}(g)\tau \sum_{j=0}^{\infty} \frac{(\mu+2\beta)^{j}}{j!} (k-1) F_k \chi^{k+j-2} \\
&+ \Omega^2 \bar{I}_0(g) \frac{\tau}{12} \sum_{j=0}^{\infty} \frac{(\mu+\beta)^{j}}{j!} U_k \chi^{k+j} + \Omega^2 \bar{I}_1(g) \frac{\tau^3}{12} \sum_{j=0}^{\infty} \frac{(\mu+2\beta)^{j}}{j!} F_k \chi^{k+j} \Big\} = 0
\end{aligned} \tag{16a}$$

$$\begin{aligned}
&\sum_{k=0}^{\infty} \Big\{ \overline{B}(g) \sum_{j=0}^{\infty} \frac{(\mu+2\beta)^{j+1}}{j!} (k+\nu) U_k \chi^{k+j-1} + \overline{D}(g)\tau \sum_{j=0}^{\infty} \frac{(\mu+3\beta)^{j+1}}{j!} (k+\nu) F_k \chi^{k+j-1} \\
&+ \overline{B}(g) \sum_{j=0}^{\infty} \frac{(\mu+2\beta)^{j}}{j!} (k-1)(k-\nu) U_k \chi^{k+j-2} + \overline{D}(g)\tau \sum_{j=0}^{\infty} \frac{(\mu+3\beta)^{j}}{j!} (k-1)(k-\nu) F_k \chi^{k+j-2} \\
&+ (1-\nu)\overline{B}(g) \sum_{j=0}^{\infty} \frac{(\mu+2\beta)^{j}}{j!} (k-1) U_k \chi^{k+j-2} + (1-\nu)\overline{D}(g)\tau \sum_{j=0}^{\infty} \frac{(\mu+3\beta)^{j}}{j!} (k-1) F_k \chi^{k+j-2} \\
&- \frac{\kappa^2 (1-\nu)\overline{A}(g)}{2\tau} \sum_{j=0}^{\infty} \frac{(\mu+\beta)^{j}}{j!} (F_k \chi^{k+j} + k W_k \chi^{k+j-1}) \\
&+ \Omega^2 \frac{\tau^2}{12} \bar{I}_1(g) \sum_{j=0}^{\infty} \frac{(\mu+2\beta)^{j}}{j!} U_k \chi^{k+j} + \Omega^2 \bar{I}_2(g) \frac{\tau^3}{12} \sum_{j=0}^{\infty} \frac{(\mu+3\beta)^{j}}{j!} F_k \chi^{k+j} \Big\} = 0
\end{aligned} \tag{16b}$$

$$\sum_{k=0}^{\infty}\left\{\overline{A}(g)\sum_{j=0}^{\infty}\frac{(\mu+\beta)^j}{j!}k[F_k\chi^{k+j-1}+(k-1)W_k\chi^{k+j-2}]+\overline{A}(g)\sum_{j=0}^{\infty}\frac{(\mu+\beta)^j}{j!}[F_k\chi^{k+j-1}+kW_k\chi^{k+j-2}]\right.$$
$$+\overline{A}(g)\sum_{j=0}^{\infty}\frac{(\mu+\beta)^{j+1}}{j!}[F_k\chi^{k+j}+kW_k\chi^{k+j-1}]+\frac{\tau^2}{6\kappa^2(1-\nu)}\Omega^2\overline{I}_0(g)\sum_{j=0}^{\infty}\frac{(\mu+\beta)^j}{j!}W_k\chi^{k+j}$$
$$\left.-\frac{K_w\tau^2}{6\kappa^2(1-\nu)}W_k\chi^k+\frac{K_s\tau^2}{6\kappa^2(1-\nu)}k^2W_k\chi^{k-2}\right\}=0 \tag{16c}$$

Simplifying Eq. (16) and rearranging, the equations of motion can be transformed into the following recurrence equation:

$$U_{k+2}=\frac{1}{\overline{A}(g)(k+3)(k+1)}\left\{-\overline{A}(g)\sum_{j=1}^{k}\frac{(\mu+\beta)^j}{j!}(k-j+3)(k-j+1)U_{k-j+2}\right.$$
$$-\overline{A}(g)\sum_{j=0}^{k}\frac{(\mu+\beta)^{j+1}}{j!}[k-j+1+\nu]U_{k-j+1}-\overline{B}(g)\tau\sum_{j=0}^{k}\frac{(\mu+2\beta)^{j+1}}{j!}[k-j+1+\nu]F_{k-j+1}$$
$$-\overline{B}(g)\tau\sum_{j=0}^{k}\frac{(\mu+2\beta)^j}{j!}(k-j+3)(k-j+1)F_{k-j+2}$$
$$\left.-\Omega^2\frac{\tau}{12}\overline{I}_1(g)\sum_{j=0}^{k}\frac{(\mu+\beta)^j}{j!}U_{k-j}-\Omega^2\overline{I}_2(g)\frac{\tau^3}{12}\sum_{j=0}^{k}\frac{(\mu+2\beta)^j}{j!}F_{k-j}\right\} \tag{17a}$$

$$F_{k+2}=\frac{\overline{A}(g)}{[\overline{D}(g)\overline{A}(g)-\overline{B}(g)^2]\tau(k+3)(k+1)}$$
$$\left\{\tau\sum_{j=1}^{k}\left(\frac{\overline{B}(g)^2}{\overline{A}(g)}\frac{(\mu+2\beta)^j}{j!}-\overline{D}(g)\frac{(\mu+3\beta)^j}{j!}\right)(k-j+3)(k-j+1)F_{k-j+2}\right.$$
$$+\overline{B}(g)\sum_{j=0}^{k}\left(\frac{(\mu+\beta)^{j+1}}{j!}-\frac{(\mu+2\beta)^{j+1}}{j!}\right)[k-j+1+\nu]U_{k-j+1}$$
$$+\tau\sum_{j=0}^{k}\left(\frac{\overline{B}(g)^2}{\overline{A}(g)}\frac{(\mu+2\beta)^{j+1}}{j!}-\overline{D}(g)\frac{(\mu+3\beta)^{j+1}}{j!}\right)[k-j+1+\nu]F_{k-j+1}$$
$$+\overline{B}(g)\sum_{j=1}^{k}\left(\frac{(\mu+\beta)^j}{j!}-\frac{(\mu+2\beta)^j}{j!}\right)(k-j+3)(k-j+1)U_{k-j+2}$$
$$+\frac{\kappa^2(1-\nu)}{2\tau}\overline{A}(g)\sum_{j=0}^{k}\frac{(\mu+\beta)^j}{j!}F_{k-j}+\frac{\kappa^2(1-\nu)}{2\tau}\overline{A}(g)\sum_{j=0}^{k}\frac{(\mu+\beta)^j}{j!}(k-j+1)W_{k-j+1}$$
$$-\Omega^2\overline{I}_3(g)\frac{\tau^3}{12}\sum_{j=0}^{k}\frac{(\mu+3\beta)^j}{j!}F_{k-j}+\frac{\overline{B}(g)}{\overline{A}(g)}\Omega^2\frac{\tau}{12}\overline{I}_1(g)\sum_{j=0}^{k}\frac{(\mu+\beta)^j}{j!}U_{k-j}$$
$$\left.+\Omega^2\frac{\tau^2}{12}\overline{I}_2(g)\sum_{j=0}^{k}\frac{(\mu+2\beta)^j}{j!}\left(\frac{\overline{B}(g)}{\overline{A}(g)}\tau F_{k-j}-U_{k-j}\right)\right\} \tag{17b}$$

$$W_{k+2}=\frac{6\kappa^2(1-\nu)}{K_s\tau^2+6\overline{A}(g)\kappa^2(1-\nu)}\frac{1}{(k+2)^2}\left\{-\overline{A}(g)\sum_{j=0}^{k}\frac{(\mu+\beta)^{j+1}}{j!}F_{k-j}\right.$$
$$-\overline{A}(g)\sum_{j=0}^{k}\frac{(\mu+\beta)^{j+1}}{j!}(k-j+1)W_{k-j+1}-\overline{A}(g)\sum_{j=0}^{k}\frac{(\mu+\beta)^j}{j!}(k-j+2)F_{k-j+1}$$
$$\left.-\overline{A}(g)\sum_{j=1}^{k}\frac{(\mu+\beta)^j}{j!}(k-j+2)^2W_{k-j+2}-\frac{\tau^2\Omega^2\overline{I}_1(g)}{6\kappa^2(1-\nu)}\sum_{j=0}^{k}\frac{(\mu+\beta)^j}{j!}W_{k-j}+\frac{K_w\tau^2}{6\kappa^2(1-\nu)}W_k\right\} \tag{17c}$$

3.2 Imposing the boundary conditions

By substituting Eq. (15) into the boundary condition Eq. (13), the transformed form of this equation around $\chi_0 = 0$ may be obtained as:

Free edge :

$$\begin{aligned} &M_r\big|_{r=1} = \bar{B}(g)\sum_{k=0}^{\infty}(k+\nu)U_k + \tau e^{\beta}\bar{D}(g)\sum_{k=0}^{\infty}(k+\nu)F_k = 0, \\ &N_r\big|_{r=1} = \bar{A}(g)\sum_{k=0}^{\infty}(k+\nu)U_k + \tau e^{\beta}\bar{B}(g)\sum_{k=0}^{\infty}(k+\nu)F_k = 0, \\ &Q_r\big|_{r=1} = \sum_{k=0}^{\infty}F_k + \sum_{k=0}^{\infty}kW_k = 0 \end{aligned} \tag{18a}$$

Simply – supported edge :

$$\begin{aligned} &u\big|_{r=1} = \sum_{k=0}^{\infty}U_k = 0, \qquad W\big|_{r=1} = \sum_{k=0}^{\infty}W_k = 0, \\ &M_r\big|_{r=1} = \bar{B}(g)\sum_{k=0}^{\infty}(k+\nu)U_k + \tau e^{\beta}\bar{D}(g)\sum_{k=0}^{\infty}(k+\nu)F_k = 0 \end{aligned} \tag{18b}$$

Clamped edge:

$$u\big|_{r=1} = \sum_{k=0}^{\infty}U_k = 0, \qquad w\big|_{r=1} = \sum_{k=0}^{\infty}W_k = 0, \qquad \psi_r\big|_{r=1} = \sum_{k=0}^{\infty}F_k = 0 \tag{18c}$$

Based on Eq. (18), three edge conditions are available at $\chi = 1$, that may be employed in solving Eq. (12) and consequently, determination of u_0, ψ and w. Moreover, three additional conditions are required that may be extracted from the regularity conditions at the center of the circular plate. The symmetric vibration modes correspond to the following assumption for the moderately thick plate:

$$\begin{aligned} &u\big|_{r=0} = 0 \qquad \rightarrow U_0 = 0 \\ &\psi\big|_{r=0} = 0 \qquad \rightarrow F_0 = 0 \\ &Q_r\big|_{r=0} = 0 \qquad \rightarrow W_1 = 0 \end{aligned} \tag{19}$$

By substituting U_i, W_i and F_i (i=2,..., n+2) from Eq. (17) into Eq. (18) and applying the regularity conditions, Eq. (19), the following equations are resulted:

$$\begin{aligned} &\mathrm{X}_{11}^{(n)}(\Omega)U_1 + \mathrm{X}_{12}^{(n)}(\Omega)\ W_0 + \mathrm{X}_{13}^{(n)}(\Omega)\ F_1 = 0 \\ &\mathrm{X}_{21}^{(n)}(\Omega)\ U_1 + \mathrm{X}_{22}^{(n)}(\Omega)\ W_0 + \mathrm{X}_{23}^{(n)}(\Omega)\ F_1 = 0 \\ &\mathrm{X}_{31}^{(n)}(\Omega)\ U_1 + \mathrm{X}_{32}^{(n)}(\Omega)\ W_0 + \mathrm{X}_{33}^{(n)}(\Omega)\ F_1 = 0 \end{aligned} \tag{20}$$

where X_{ij} are closed-form polynomials of Ω corresponding to nth term. Therefore, they represent closed-form series expressions. Eq. (20) can be expressed in the following matrix form:

$$\begin{bmatrix} X_{11}^{(n)}(\Omega) & X_{12}^{(n)}(\Omega) & X_{13}^{(n)}(\Omega) \\ X_{21}^{(n)}(\Omega) & X_{22}^{(n)}(\Omega) & X_{23}^{(n)}(\Omega) \\ X_{31}^{(n)}(\Omega) & X_{32}^{(n)}(\Omega) & X_{33}^{(n)}(\Omega) \end{bmatrix} \begin{Bmatrix} U_1 \\ W_0 \\ F_1 \end{Bmatrix} = 0 \tag{21}$$

Existence of a non-trivial solution require that:

$$\begin{vmatrix} X_{11}^{(n)}(\Omega) & X_{12}^{(n)}(\Omega) & X_{13}^{(n)}(\Omega) \\ X_{21}^{(n)}(\Omega) & X_{22}^{(n)}(\Omega) & X_{23}^{(n)}(\Omega) \\ X_{31}^{(n)}(\Omega) & X_{32}^{(n)}(\Omega) & X_{33}^{(n)}(\Omega) \end{vmatrix} = 0 \tag{22}$$

By solving this equation, the non-dimensional natural frequencies will be achieved. In this paper, *Newton-Raphson* method is used to solve the final equation of the non-dimensional natural frequencies. In the present study, a 0.0001 relative error parameter is chosen as a convergence criterion.

$$\frac{\left|\Omega_j^{(i+1)} - \Omega_j^{(i)}\right|}{\left|\Omega_j^{(i)}\right|} \leq \varepsilon \qquad , j = 1,2,3,...,n \tag{23}$$

where i is the iteration counter.

4 RESULTS AND DISCUSSIONS

Present section contains both comparative and new results. Although the first two examples are mainly verification examples, almost all examples contain new results that may be used as verification bases for the future researches.

Example 1: As a verification example, a one-directional transversely functionally graded circular plate with the following material properties is considered: $E_m = 70$ GPa, $\rho_m = 2700$ kg/m^3, $E_c = 380$ GPa, $\rho_c = 3800$ kg/m^3. The plate has no elastic foundation and its outer edge is free. The first two natural frequencies of the mentioned plate are calculated and compared with results reported by Hosseini-Hashemi et al. [23] and Irie et al. [24] in Table 1. Results of all references have been computed based on the first-order shear-deformation plate theory but with different analytical approaches. Results of reference [24] were obtained for pure metallic and pure ceramic plates. Results of the three approaches are almost coincident. This confirms the high accuracy of the proposed approach. As it may be expected, the natural frequencies increase due to an increase in the power law exponent g.

Example 2: In the next stage, results of circular plates with heterogeneous materials whose heterogeneity is along either the radial or axial direction are verified. To this end, present results are compared with results of Gupta et al. [25] for radially-graded plates and results of Hosseini-Hashemi et al. [23] for transversely-graded circular plates.

Table 1
A comparison between the first two natural frequencies calculated for various gradient indices of FGM circular plates with free edges ($\tau = 0.25$)

Natural frequency	Approach	Fully metallic				Fully ceramic			
		$g=10^{-3}$	$g=10^{-4}$	$g=10^{-5}$	$g=10^{-6}$	$g=10^{2}$	$g=10^{3}$	$g=10^{4}$	$g=10^{5}$
Ω_1	Present	4.22077	4.21066	4.20964	4.20953	8.18787	8.25915	8.26652	8.26736
	Ref. [23]	4.22077	4.21066	4.20964	4.20953	8.18787	8.25915	8.26652	8.26736
	Ref. [24]	4.20953				8.26736			
Ω_2	Present	14.6019	14.5688	14.5653	14.5652	28.3073	28.3822	28.3890	28.6055
	Ref. [23]	14.6018	14.5688	14.5653	14.5652	28.3082	28.3823	28.3890	28.6055
	Ref. [24]	14.5652				28.6055			

Table 2
A comparison between the first two natural frequencies (in Hz) determined by different approaches for plates with clamped edges and different geometric and material parameters

		Approach	$\mu=\eta=-0.5$			$\mu=\eta=0$			$\mu=\eta=1$		
			$\tau=0.01$	$\tau=0.1$	$\tau=0.2$	$\tau=0.01$	$\tau=0.1$	$\tau=0.2$	$\tau=0.01$	$\tau=0.1$	$\tau=0.2$
$g=0$	Ω_1	Present	23.292	226.725	421.497	24.045	243.779	453.189	29.075	282.733	524.532
		Ref. [25]	---	226.733	421.525	---	243.808	453.212	---	282.716	524.570
	Ω_2	Present	95.34076	875.346	1449.097	97.437	894.572	1481.720	102.347	939.011	1554.205
		Ref. [25]	---	875.331	1449.767	---	894.530	1481.709	---	939.044	1554.172
$g=1$	Ω_1	Present	34.922	341.173	640.05413	37.552	366.82	688.04	43.594	425.401	796.109
		Ref. [23]	---	---	---	37.5518	366.905	688.625	---	---	---
	Ω_2	Present	142.962	1325.662	2234.7088	146.106	1355.3	2284.4	153.468	1421.829	2394.746
		Ref. [23]	---	---	---	146.107	1355.70	2288.44	---	---	---
$g=3$	Ω_1	Present	38.529	376.618	707.503	41.403	404.927	760.549	48.097	469.639	880.248
	Ω_2	Present	157.731	1465.422	2478.164	161.199	1497.524	2532.499	169.32	1571.854	2656.018

Table 3
A comparison between the first two natural frequencies (in Hz) determined by different approaches for plates with simply-supported edges and different geometric and material parameters

		Approach	$\mu=\eta=-0.5$			$\mu=\eta=0$			$\mu=\eta=1$		
			$\tau=0.01$	$\tau=0.1$	$\tau=0.2$	$\tau=0.01$	$\tau=0.1$	$\tau=0.2$	$\tau=0.01$	$\tau=0.1$	$\tau=0.2$
$g=0$	Ω_1	Present	11.846	117.561	229.271	12.101	120.012	234.307	12.552	124.518	243.345
		Ref. [25]	---	117.572	229.282	---	120.035	234.294	---	124.538	243.383
	Ω_2	Present	72.024	685.233	1212.643	72.842	692.531	1225.904	74.937	712.1301	1259.646
		Ref[25]	---	685.212	1212.67	---	692.517	1225.922	---	712.141	1259.648
$g=1$	Ω_1	Present	18.940	187.817	366.599	19.453	192.181	375.49	20.183	200.265	391.574
		Ref. [23]	---	---	---	18.1443	180.081	352.383	---	---	---
	Ω_2	Present	109.160	1041.751	1858.564	110.02	1051.4	1876.2	113.2112	1079.876	1925.118
		Ref. [23]	---	---	---	109.220	1043.97	1868.96	---	---	---
$g=3$	Ω_1	Present	20.225	200.676	392.320	20.662	205.071	401.257	21.475	213.182	417.392
	Ω_2	Present	119.793	1145.627	2052.531	121.015	1157.323	2073.748	124.400	1189.098	2128.776

Table 4
A comparison between the first two natural frequencies (in Hz) determined by different approaches for plates with free edges and different geometric and material parameters.

		Approach	$\mu=\eta=-0.5$			$\mu=\eta=0$			$\mu=\eta=1$		
			$\tau=0.01$	$\tau=0.1$	$\tau=0.2$	$\tau=0.01$	$\tau=0.1$	$\tau=0.2$	$\tau=0.01$	$\tau=0.1$	$\tau=0.2$
$g=0$	Ω_1	Present	22.7692	224.226	429.721	22.075216	217.46905	417.14345	21.079	207.69109	398.51442
		Ref. [25]	---	224.185	429.680	---	217.473	417.107	---	207.704	398.503
	Ω_2	Present	94.552	887.073	1531.626	94.207806	883.83021	1525.8592	94.254	883.83379	1523.891
		Ref. [25]	---	887.054	1531.659	---	883.826	1525.883	---	883.826	1523.929
$g=1$	Ω_1	Present	34.136792	336.422	645.86205	33.097	326.23383	626.59509	31.606122	311.47359	597.94164
	Ω_2	Present	141.77348	1336.141	2323.6880	141.248	1331.0921	2312.5825	141.31337	1330.814	2299.3046
	Ω_2	Present	37.665415	371.432	714.42950	36.517267	360.19274	693.18932	34.869457	343.92261	661.69672
	Ω_2	Present	156.42764	1477.616	2583.1379	155.836	1472.092	2572.173	155.919	1471.948	2564.086

Table 5
Influence of various material heterogeneity, geometric, thickness, and foundation parameters of a clamped two-directional functionally graded circular plate resting on an elastic foundation

			g=0	g=1	g=3	g=5	g=10	g=20	g=35	g=50	g=100
$\tau = 0.1$	Baseline	Ω_1	5.0616	7.6161	8.4075	8.7628	9.1902	9.5058	9.6742	9.7486	9.8412
		Ω_2	18.493	28.1271	31.0931	32.3786	33.8909	34.9882	35.5679	35.8231	36.1397
	$\mu = \eta = 0.5$	Ω_1	5.4482	8.1974	9.0496	9.4321	9.8922	10.2319	10.4130	10.4932	10.5929
		Ω_2	19.0147	28.7927	31.8298	33.1461	34.6946	35.8181	36.4116	36.6728	36.9970
	$\mu = \eta = -0.5$	Ω_1	4.7075	7.0838	7.8197	8.1501	8.5475	8.8409	8.9974	9.0666	9.1528
		Ω_2	18.1748	27.5247	30.4266	31.6841	33.1634	34.2368	34.8038	35.0534	35.3631
	$\beta = 0.5$	Ω_1	7.4182	11.2058	12.3699	12.8846	13.4991	13.9503	14.1902	14.2961	14.4278
		Ω_2	23.6615	36.0577	39.8999	41.5114	43.3685	44.6941	45.3882	45.6924	46.0687
	$\beta = -0.5$	Ω_1	3.47298	5.2238	5.7613	6.0045	6.2991	6.5179	6.6349	6.6868	6.7513
		Ω_2	14.3023	21.5728	23.8285	24.8273	26.0183	26.8918	27.3561	27.5610	27.8158
	$K_w = 50$	Ω_1	9.7787	10.7764	11.1491	11.3601	11.6425	11.8657	11.98894	12.0441	12.1134
		Ω_2	20.3447	29.1244	31.9299	33.1633	34.6248	35.6907	36.25524	36.5039	36.8128
	$K_s = 20$	Ω_1	14.2291	14.5066	14.5745	14.6719	14.8358	14.9809	15.06476	15.1031	15.1516
		Ω_2	34.9988	39.1313	40.6442	41.4315	42.4457	43.2269	43.65185	43.8412	44.0779
$\tau = 0.2$	Baseline	Ω_1	4.7048	7.1424	7.8957	8.2189	8.5970	8.8702	9.0142	9.0775	9.1560
		Ω_2	15.3825	23.7074	26.2912	27.3079	28.4299	29.2036	29.6008	29.7733	29.9855
	$\mu = \eta = 0.5$	Ω_1	5.0606	7.6812	8.4921	8.8400	9.2469	9.5409	9.6959	9.7639	9.8484
		Ω_2	15.7442	24.2615	26.9069	27.9482	29.0974	29.8897	30.2964	30.4731	30.6904
	$\mu = \eta = -0.5$	Ω_1	4.3758	6.6447	7.3449	7.6452	7.9966	8.2503	8.3841	8.4429	8.5158
		Ω_2	15.0507	23.1997	25.7271	26.7211	27.8181	28.5744	28.9627	29.1314	29.3389
	$\beta = 0.5$	Ω_1	6.5394	10.0162	11.0825	11.5205	12.0198	12.3732	12.5573	12.6377	12.7372
		Ω_2	18.0568	28.1315	31.2408	32.3943	33.6162	34.4309	34.8416	35.0185	35.2348
	$\beta = -0.5$	Ω_1	3.3313	5.0377	5.5607	5.7910	6.0656	6.2668	6.3737	6.4209	6.4796
		Ω_2	12.6442	19.3114	21.3844	22.2413	23.2189	23.9113	24.2722	24.42997	24.625
	$K_w = 50$	Ω_1	9.5594	10.4123	10.7396	10.9192	11.1553	11.3392	11.4396	11.4844	11.5406
		Ω_2	17.4301	24.8454	27.247	28.2081	29.278	30.0203	30.4026	30.5688	30.7736
	$K_s = 20$	Ω_1	13.7956	13.9962	14.0473	14.1223	14.2487	14.36	14.424	14.4532	14.4901
		Ω_2	32.587	35.3412	36.4635	37.0011	37.6577	38.1433	38.4014	38.5152	38.6565

For cases where the material properties vary in the transverse direction, the material properties are similar to those defined in the foregoing example. The numerical results have been reported and computed for the first two modes of vibration to investigate effect of the heterogeneity parameter μ, density parameter η, and thickness parameter τ on the natural frequencies. Results are obtained for $g = 0,1,3$, $\mu = \eta = -0.5,0,0.5$, $\tau = 0.01,0.1,0.2$, and $\beta = 0$ and are listed in Tables 2 to Tables 4 for circular plates with clamped, simply-supported, and free edges, respectively. Therefore, the results are computed for thin $(\tau = 0.01)$, relatively thick $(\tau = 0.1)$, and thick $(\tau = 0.2)$, plates. Results of reference [25] correspond to g=0 whereas results of reference [23] are related to $\mu = \eta = 0$ and plates with clamped or simply-supported edges. There is an excellent agreement between present results and results of references [23] and [25], especially, for plates with clamped edges. The discrepancies are especially negligible for higher natural frequencies. As it may be expected, for plates with less restrained edge conditions, the overall rigidity of the plate and subsequently, the natural frequencies are lower. However, since the circular plates with free edges are indeed unrestrained, this conclusion does not hold. As it may be readily noted from Tables 2 to Tables 4 majority of the present results are new and can be used for future comparative studies.

Example 3: To evaluate influences of various parameters: geometric parameters, thickness variation, material gradient indices, edge conditions, and coefficients of the *Winkler-Pasternak* foundation, a sensitivity analysis is carried out for thick $(\tau = 0.2)$ and relatively thick $(\tau = 0.1)$ clamped two-directional functionally graded circular plates. A case associated with an isotropic uniform-thickness plate with clamped edge is considered as a baseline to assess effects of the parameters individually. Results of the sensitivity analysis are shown in Table 5. Due to the specific definition of the dimensionless natural frequency, although the natural frequencies are expected to increase with an increase in the plate thickness, they are lower for thicker plates. However, effects of other parameters on the natural frequency may be observed directly. Results reveal that since greater power-law indices (g) lead to an FGM mixture with a greater ceramic volume fraction, the natural frequencies are greater for greater g values. Higher positive μ and η values increase the plate rigidity in the radial direction so that influence of the clamping support may affect regions that are far from the edges more pronouncedly. Therefore, the bending rigidity and subsequently, the natural frequencies increase. Greater β values lead to cross sections with greater heights. Hence, they increase the natural frequencies.

Presence of the elastic foundation reduces the plate movability and subsequently, increases the apparent (extensional or bending) rigidity of the plate and increases the natural frequencies. Results confirm that effect of *Pasternak* coefficient of the elastic foundation on the natural frequencies of the plate is more remarkable in comparison with an identical *Winkle*r coefficient.

Example 4: In the present example, variations of the natural frequencies and their rates with respect to the power-law index of the transverse variations of the material properties (g) are studied for various cases. The thickness ratio of the plate is assumed to $\tau = 0.1$. In this regard, simultaneous effects of the power-law index and parameters such as variations of the cross section in the radial direction and *Winkler* or *Pasternak* coefficients of the elastic foundation on the first two natural frequencies of the plate are investigated.

Results are depicted in Figs. 2 and 3 for the first and second natural frequencies of a simply-supported plate resting on an elastic foundation, respectively. Results of a plate with a free outer edge are shown in Figs. 4 and 5. It may be easily verified that the cases with $g = 0$ and $g = \infty$ correspond to pure metallic and pure ceramic plates, respectively.

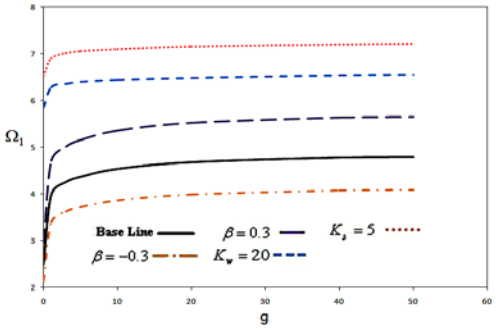

Fig. 2
Simultaneous effects of variations of the cross section in the radial direction, *Winkler* or *Pasternak* coefficients of the elastic foundation, and effect of the power-law index of the material mixture on the first natural frequency of a simply-supported plate.

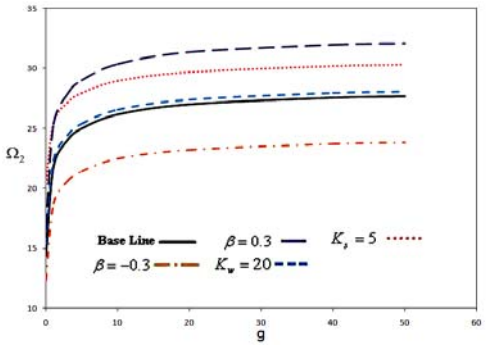

Fig. 3
Simultaneous effects of variations of the cross section in the radial direction, *Winkler* or *Pasternak* coefficients of the elastic foundation, and effect of the power-law index of the material mixture on the second natural frequency of a simply-supported plate.

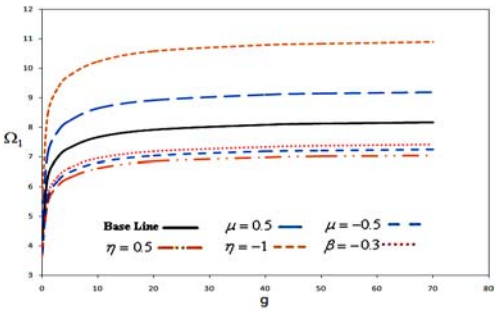

Fig. 4
Simultaneous effects of variations of the cross section in the radial direction, *Winkler* or *Pasternak* coefficients of the elastic foundation, and effect of the power-law index of the material mixture on the first natural frequency of a plate with a free edge.

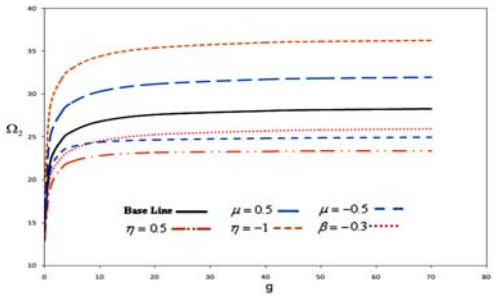

Fig. 5
Simultaneous effects of variations of the cross section in the radial direction, *Winkler* or *Pasternak* coefficients of the elastic foundation, and effect of the power-law index of the material mixture on the second natural frequency of a plate with a free edge.

Results illustrated in Figs. 2-5 reveal that for plates fabricated from a mixture whose power-law exponents are almost zero (metallic plates), the natural frequency is the minimum. The natural frequency increases asymptotically as the power-law exponent increases so that increasing the power-law exponent of the material beyond 10 leads to an ignorable increase/enhancement in the natural frequencies of the plate. As it may be seen from Figs. 2-5, in low values of the power-law exponent, the frequencies vary with higher rates. As it may be expected, higher frequencies may be achieved for greater μ and smaller η values. In other word, while increasing the stiffness of the cross sections of the circular plate in the radial direction may increase the natural frequencies of the plate, the natural frequencies are increased when the mass density of the mixture of the materials is reduced in the radial direction. Figs. 6 and 7 illustrate influence of exponent of variations of the elasticity modulus in the radial direction on the natural frequencies of a circular plate with a simply-supported edge. As it may be readily observed, the natural frequencies increase with an increase in μ. However, in contrast to graphs plotted for evaluating effects of the power-law exponent (Figs. 2-7), the curves do not exhibit an asymptotic behavior. Finally, from the presented results, it may be inferred that the reduction in rigidity due to reduction of the sections heights may be somewhat compensated by the power or exponential laws exponents of the material properties in the radial, transverse or both directions.

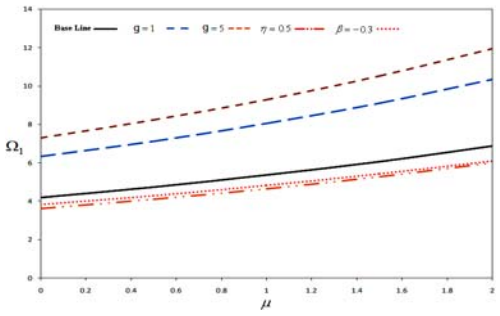

Fig. 6
Influence of exponent of variations of the elasticity modulus in the radial direction on the first natural frequency of a circular plate with a simply-supported edge.

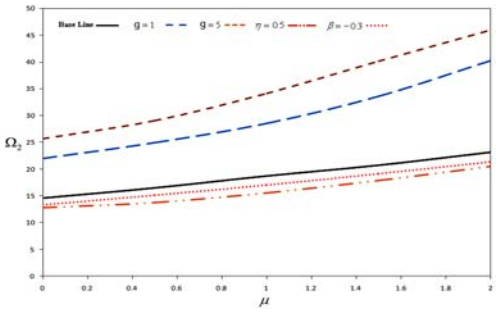

Fig. 7
Influence of exponent of variations of the elasticity modulus in the radial direction on the second natural frequency of a circular plate with a simply-supported edge.

5 CONCLUSIONS

In the present paper, a closed-form semi-analytical solution is employed to investigate free vibration of two-directional functionally graded circular plates having various edge restraints and variable thickness resting on *Winkler-Pasternak* elastic foundations. In this regard, the differential transform technique is utilized. A comprehensive sensitivity analysis consists of evaluating influences of various parameters is performed. The proposed close-form solution covers complex combinations of the material properties heterogeneity in both radial and transverse directions, thickness variations, edge restraints, and coefficients of the two-parameter elastic foundation. Comparisons made with the special cases available in literature, have verified the accuracy of the proposed solution. As the results show, degradations caused by a group of the factors (e.g., the geometric parameters) in the vibration behavior of the structure may be compensated by a group of factors of different nature (e.g, the material heterogeneity parameters). Moreover, employing the elastic foundation leads to higher natural frequencies and postponing the resonances.

REFERENCES

[1] Zhou D., Lo S.H., Au F.T.K., Cheung Y.K., 2006, Three dimensional free vibration of thick circular plates on Pasternak foundation, *Journal of Sound and Vibration* **292**: 726-741.

[2] Hosseini-Hashemi Sh., Rokni Damavandi Taher H., Omidi M., 2008, 3-D free vibration analysis of annular plates on Pasternak elastic foundation via p-Ritz method, *Journal of Sound and Vibration* **311**: 1114-1140.

[3] Ramaiah G.K., Vijayakumar K., 1973, Natural frequencies of polar orthotropic annular plates, *Journal of Sound and Vibration* **26**: 517-531.

[4] Narita Y., 1984, Natural frequencies of completely free annular and circular plates having polar orthotropy, *Journal of Sound and Vibration* **92**: 33-38.

[5] Lin C.C., Tseng C.S., 1998, Free vibration of polar orthotropic laminated circular and annular plates, *Journal of Sound and Vibration* **209**: 797-810.

[6] Prakash T., Ganapathi M., 2006, Asymmetric flexural vibration and thermoelastic stability of FGM circular plates using finite element method, *Composites Part B* **37**: 642–649.

[7] Efraim E., Eisenberger M., 2007, Exact vibration analysis of variable thickness thick annular isotropic and FGM plates, *Journal of Sound and Vibration* **299**: 720-738.

[8] Nie G.J., Zhong Z., 2007, Semi-analytical solution for three-dimensional vibration of functionally graded circular plates, *Computer Methods in Applied Mechanics and Engineering* **196**: 4901-4910.

[9] Dong C.Y., 2008, Three-dimensional free vibration analysis of functionally graded annular plates using the Chebyshev-Ritz method, *Materials and Design* **29**: 1518-1525.
[10] Malekzadeh P., 2009, Three-dimensional free vibration analysis of thick functionally graded plates on elastic foundations, *Composite Structures* **89**: 367-373.
[11] Wang Y., Xu R.Q., Ding H.J., 2009, Free axisymmetric vibration of FGM circular plates, *Applied Mathematics and Mechanics* **30**: 1077-1082.
[12] Nie G.J., Zhong Z., 2010, Dynamic analysis of multi-directional functionally graded annular plates, *Applied Mathematical Modelling* **34**: 608-616.
[13] Arikoglu A., Ozkol I., 2005, Solution of boundary value problems for integro-differential equations by using differential transform method, *Applied Mathematics and Computation* **168**: 1145-1158.
[14] Chen C.K., Ho S.H., 1998, Application of differential transformation to eigenvalue problems, *Applied Mathematics and Computation* **79**: 173-188.
[15] Malik M., Dang H.H., 1998, Vibration analysis of continuous systems by differential transformation, *Applied Mathematics and Computation* **96**: 17-26.
[16] Yeh Y.L., Jang M.J., Wang C.C., 2006, Analyzing the free vibrations of a plate using finite difference and differential transformation method, *Applied Mathematics and Computation* **178**: 493-501.
[17] Yeh Y.-L., Wang C.C., Jang M.-J., 2007, Using finite difference and differential transformation method to analyze of large deflections of orthotropic rectangular plate problem, *Applied Mathematics and Computation* **190**: 1146-1156.
[18] Yalcin H.S., Arikoglu A., Ozkol I., 2009, Free vibration analysis of circular plates by differential transformation method, *Applied Mathematics and Computation* **212**: 377-386.
[19] Shariyat M., Alipour MM., 2011, Differential transform vibration and modal stress analyses of circular plates made of two-directional functionally graded materials, resting on elastic foundations, *Archives of Applied Mechanics* **81**: 1289-1306**.**
[20] Alipour M.M., Shariyat M., Shaban M., 2010, A semi-analytical solution for free vibration of variable thickness two-directional-functionally graded plates on elastic foundations, *International Journal of Mechanics and Materials in Design* **6**: 293-304.
[21] Reddy J.N., 2007, *Theory and Analysis of Elastic Plates and Shells*, CRC/Taylor & Francis, Second edition.
[22] Reddy J.N., 2004, *Mechanics of Laminated Composite Plates and Shells: Theory and Analysis*, CRC Press, Second edition.
[23] Hosseini-Hashemi Sh., Fadaee M., Es'haghi M., 2010, A novel approach for in-plane, out-of-plane frequency analysis of functionally graded circular/annular plates, *International Journal of Mechanical Sciences* **52**: 1025-1035.
[24] Irie T., Yamada G., Takagi K., 1980, Natural Frequencies of Circular Plates, *Journal of Applied Mechanics* **47**: 652-655.
[25] Gupta U.S., Lal R., Sharma S., 2007, Vibration of non-homogeneous circular Mindlin plates with variable thickness, *Journal of Sound and Vibration* **302**: 1-17.